Supporting Information

Interface-Tailored ZnO/BDPQ-Oct Inorganic/Organic Dual Sensors for Improved Light/Gas Detection and Artificial Intelligence-Enabled Gas Recognition

Chang-Hsueh Lee[a], Zong-Liang Huang[a], Yi-Hao Cai[a], Chia-Chi Chang[b], Ting-An Lin[c], Jeih-Weih Hung[b], Chia-Feng Lin[d], Yung-Sen Lin[e], Ming-Hsien Li[a,f]*, Ming-Yu Kuo[c]*, Hsiang Chen[a]*, Yung-Hui Li[g], and Jung Han[h]

[a]Department of Applied Materials and Optoelectronic Engineering, National Chi Nan University, 54561, Nantou, Taiwan
[b]Department of Electrical Engineering, National Chi Nan University, 54561, Nantou, Taiwan
[c]Department of Applied Chemistry, National Chi Nan University, 54561, Nantou, Taiwan
[d]Department of Materials Science and Engineering, National Chung Hsing University, 402202, Taichung, Taiwan
[e]Department of Chemical Engineering, Feng Chia University, 407102, Taichung, Taiwan
[f]Department of Electro-Optical Engineering, National Formosa University, Yunlin 63201, Taiwan
[g]AI Research Center, Hon Hai Research Institute No. 32 Jihu Rd., Neihu District, Taipei, Taiwan, 114699
[h]Department of Electrical Engineering, Yale University, New Haven, CT 06511 USA

Synthesis of BDPQ-Oct:

The synthesis of BDPQ-Oct was followed the route outlined in **Figure S1**. Compound **1** was synthesized following a previously described method [S1]. A two-neck round-bottom flask, compound **1** (100 mg, 0.23 mmol) and compound **2** (99.4 mg, 0.92 mmol) were dissolved in EtOH (7.5 mL), followed by the addition of acetic acid (15 mL). The reaction mixture was stirred and heated to reflux at 120 °C for 4 hours. Upon completion, the aqueous layer was extracted with with dichloromethane, and the organic phase was dried over anhydrous $MgSO_4$. The solvent was then evaporated under reduced pressure, and the resulting crude product was subjected to purification via column chromatography using a hexane/DCM (1:1) eluent, affording BDPQ-Oct as a red solid in a yield of 32%. ^{1}H NMR (300 Hz, $CDCl_3$) δ = 0.85 (t, *J* = 8.4 Hz, 12H), 1.25 (s, 2H), 2.01-2.11 (m, *J* = 3.6 Hz, 4H), 4.64 (t, *J* = 7.2 Hz, 4H), 7.68-7.74 (m, *J* = 11.4 Hz, 2H), 7.77-7.83 (m, *J* = 3Hz, 2H), 8.18 (d, *J* = 8.1 Hz, 2H), 8.35 (d, *J* = 8.1 Hz, 2H), 8.58 (s, 2H) ppm.^{13}C NMR (75 Hz, $CDCl_3$) δ = 1.0, 14.0, 22.6, 27.1, 28.4, 29.2, 29.3, 29.7, 31.8, 41.9, 102.9, 122.5, 125.9, 127.9, 129.3, 139.1, 139.3, 139.7, 141.2 ppm. MS (EI^+) calcd. for $C_{38}H_{44}N_6$: 584.3627 ; found : 584.3630.

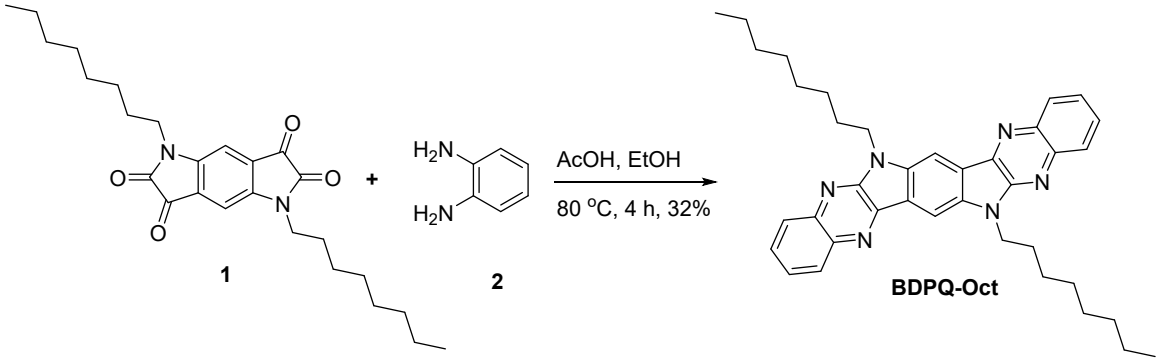

Figure S1. Synthetic reagents and conditions to BDPQ-Oct.

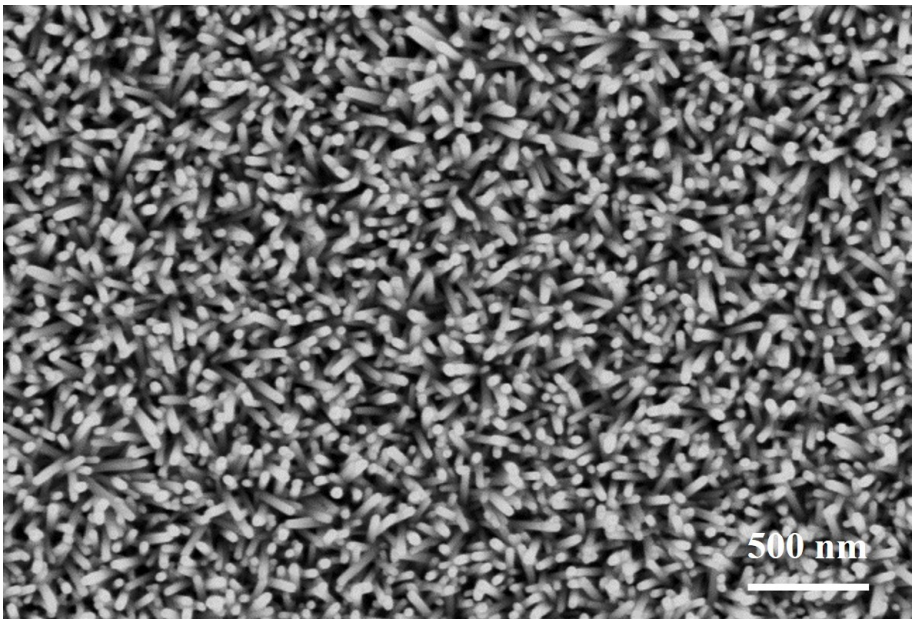

Figure S2. Top-view FESEM images of ZnO NRs.

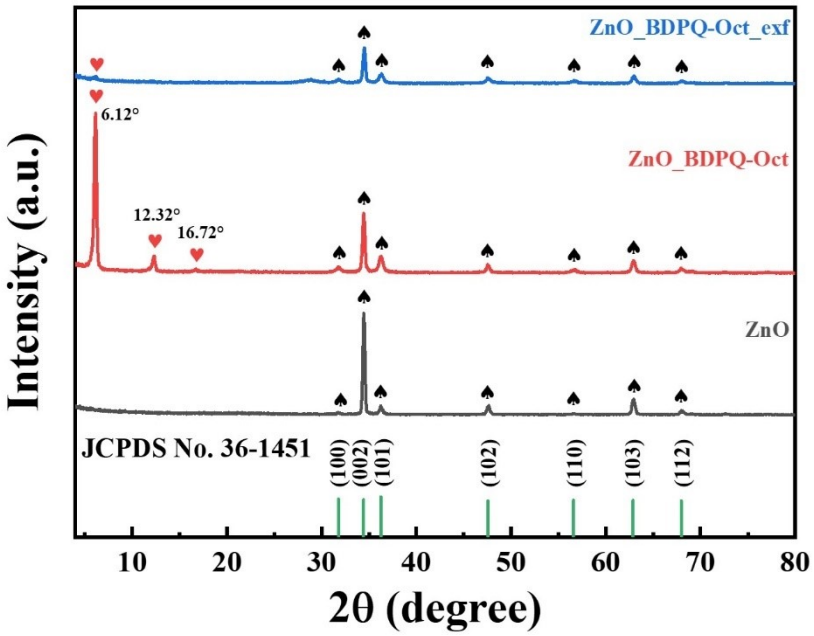

Figure S3. XRD profiles of ZnO, ZnO_BDPQ-Oct, and ZnO_BDPQ-Oct_exf device. Reference XRD profiles of ZnO (JCPDS No. 36-1451) is inserted for comparison. Characteristic XRD peaks assigned to ZnO and BDPQ-Oct are marked by ♠ and ♥, respectively.

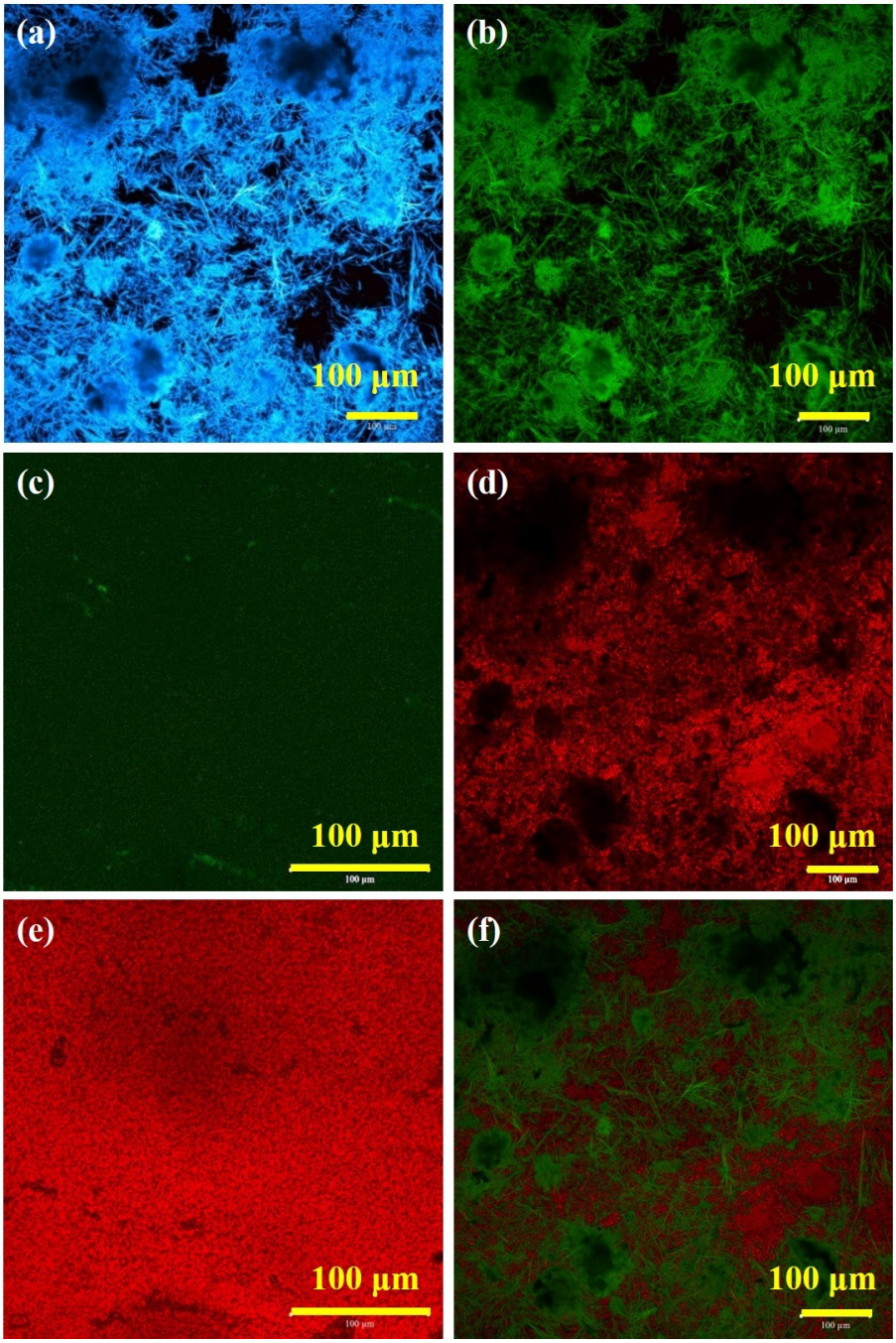

Figure S4. CLSM images of ZnO_BDPQ-Oct sample excited by (a) 488 nm laser ($\lambda_{excitation}$ = 488 nm) and (b) 555 nm laser ($\lambda_{excitation}$ = 555 nm), received the PL emission wavelength ranging from 500 to 630 nm ($\lambda_{collection}$ = 500–630 nm). (c) CLSM images of ZnO_BDPQ-Oct_exf sample under the condition of $\lambda_{excitation}$ = 555 nm and $\lambda_{collection}$ = 500–630 nm. CLSM images of (d) ZnO_BDPQ-Oct sample and (e) ZnO_BDPQ-Oct_exf sample under the condition of $\lambda_{excitation}$ = 639 nm and $\lambda_{collection}$ = 630–700 nm. (f) Overlapping CLSM image of (b) and (d).

Characterization:

At a room temperature of 25℃, we measured the photoresponsivity of different sensing devices exposed to a UV light-emitting diode (LED) (peak wavelength: 365 nm), a red LED (peak wavelength: 630 nm), and a white LED.UV, using a light sensing apparatus shown in **Figure S5(a)**. The device was placed within a probe station that connected its two electrodes to a semiconductor parameter analyzer (4155C). With a bias voltage of 5 V applied across the two electrodes, the devices were subjected to illumination from a light source that cycled on and off in 30-second intervals. The photo sensitivity and photoresponsivity of the light-sensing device was calculated using the following formulas:

$$\text{Photo sensitivity (\%)} = \frac{I_p - I_d}{I_d} \times 100\% \quad (1)$$

$$\text{Photoresponsivity (A/W)} = \frac{I_p - I_d}{P} \quad (2)$$

, where I_p and I_d are the photocurrent and dark current of the devices, respectively, and P is the power of the illumination light sources.

The gas sensing device was initially placed in a sensing chamber to evaluate its sensitivity to acetone and carbon monoxide (CO) gas. Similarly, the two electrodes of the devices were connected to a source meter (Keithley), as shown in **Figure S5(b)**. With a bias voltage of 5 V applied across the two electrodes, the device was exposed to consecutive cycles of zero gas and target gas to measure the corresponding real-time changes in resistance. Under ambient temperature of 25℃, the inflow of zero gas and target gases into the gas sensing chamber can be controlled using a mass flow controller (MFC). Once the zero gas has been introduced into the chamber and the resistance of devices had stabilized, this resistance was denoted as R_a. When 300 ppm of the target gas was introduced into the chamber, replacing the zero gas, the resistance of the devices was denoted as R_g. By repeating the gas exchange at fixed intervals, the gas sensitivity was calculated using the following equation:

$$\text{Gas sensitivity} = \frac{R_g - R_a}{R_a} \times 100\% \quad (3)$$

, where R_g and R_a are the resistance of devices exposed to the target gas and zero gas, respectively.

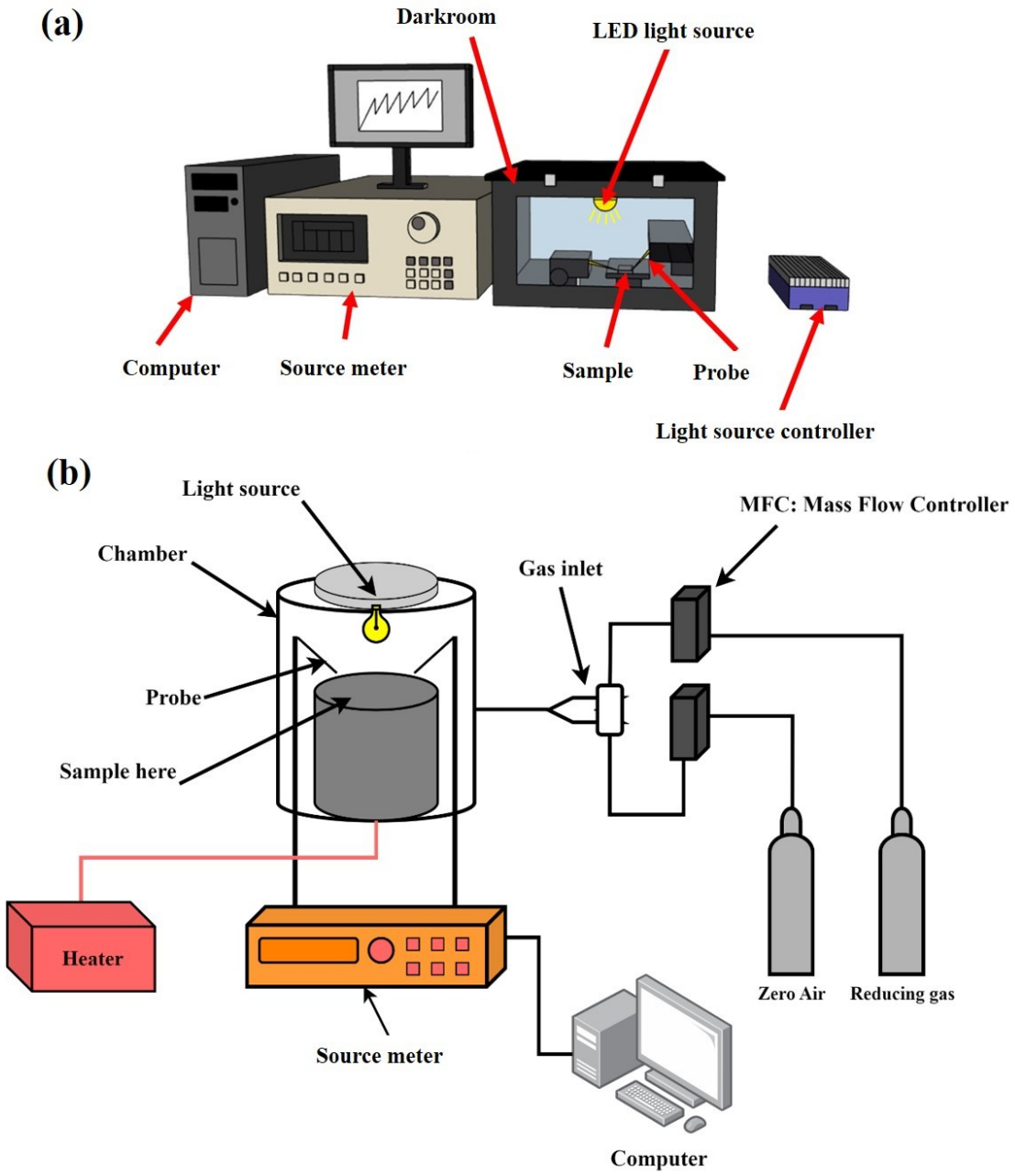

Figure S5. Schematic illustration of (a) light and (b) gas sensing apparatus.

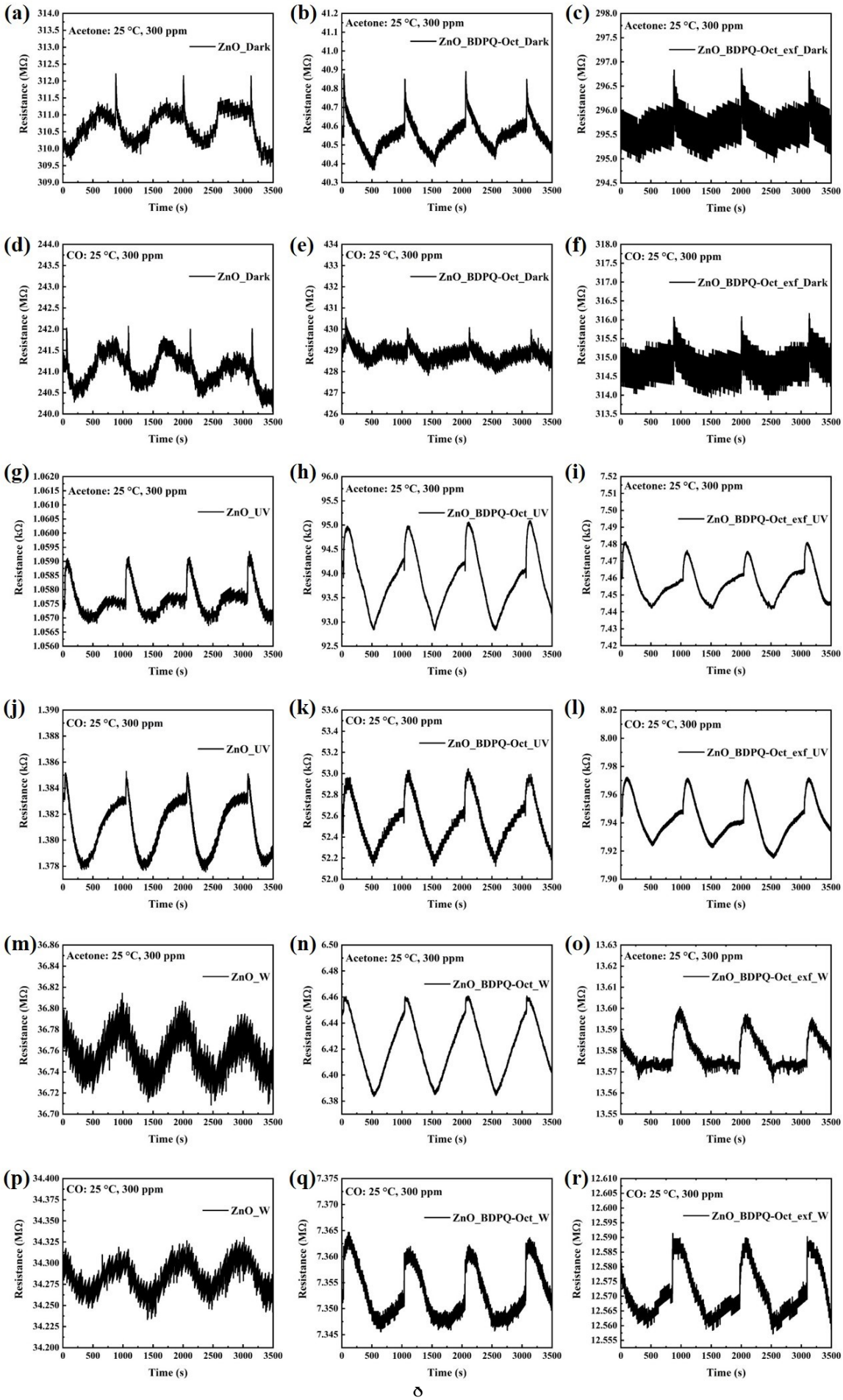
(a)
Acetone: 25 °C, 300 ppm
ZnO_Dark
Resistance (MΩ)
Time (s)
(b)
Acetone: 25 °C, 300 ppm
ZnO_BDPQ-Oct_Dark
Resistance (MΩ)
Time (s)
(c)
Acetone: 25 °C, 300 ppm
ZnO_BDPQ-Oct_exf_Dark
Resistance (MΩ)
Time (s)
(d)
CO: 25 °C, 300 ppm
ZnO_Dark
Resistance (MΩ)
Time (s)
(e)
CO: 25 °C, 300 ppm
ZnO_BDPQ-Oct_Dark
Resistance (MΩ)
Time (s)
(f)
CO: 25 °C, 300 ppm
ZnO_BDPQ-Oct_exf_Dark
Resistance (MΩ)
Time (s)
(g)
Acetone: 25 °C, 300 ppm
ZnO_UV
Resistance (kΩ)
Time (s)
(h)
Acetone: 25 °C, 300 ppm
ZnO_BDPQ-Oct_UV
Resistance (kΩ)
Time (s)
(i)
Acetone: 25 °C, 300 ppm
ZnO_BDPQ-Oct_exf_UV
Resistance (kΩ)
Time (s)
(j)
CO: 25 °C, 300 ppm
ZnO_UV
Resistance (kΩ)
Time (s)
(k)
CO: 25 °C, 300 ppm
ZnO_BDPQ-Oct_UV
Resistance (kΩ)
Time (s)
(l)
CO: 25 °C, 300 ppm
ZnO_BDPQ-Oct_exf_UV
Resistance (kΩ)
Time (s)
(m)
Acetone: 25 °C, 300 ppm
ZnO_W
Resistance (MΩ)
Time (s)
(n)
Acetone: 25 °C, 300 ppm
ZnO_BDPQ-Oct_W
Resistance (MΩ)
Time (s)
(o)
Acetone: 25 °C, 300 ppm
ZnO_BDPQ-Oct_exf_W
Resistance (MΩ)
Time (s)
(p)
CO: 25 °C, 300 ppm
ZnO_W
Resistance (MΩ)
Time (s)
(q)
CO: 25 °C, 300 ppm
ZnO_BDPQ-Oct_W
Resistance (MΩ)
Time (s)
(r)
CO: 25 °C, 300 ppm
ZnO_BDPQ-Oct_exf_W
Resistance (MΩ)
Time (s)

Figure S6. R-t responses of ZnO, ZnO_BDPQ-Oct, and ZnO_BDPQ-Oct_exf devices under various light conditions for acetone and CO gas sensing. Acetone gas sensing of (a) ZnO, (b) ZnO_BDPQ-Oct, and (c) ZnO_BDPQ-Oct_exf devices in dark conditions. CO gas sensing for (d) ZnO, (e) ZnO_BDPQ-Oct, and (f) ZnO_BDPQ-Oct_exf devices in dark conditions. Acetone gas sensing of (g) ZnO, (h) ZnO_BDPQ-Oct, and (i) ZnO_BDPQ-Oct_exf devices under UV LED illumination. CO gas sensing of (j) ZnO, (k) ZnO_BDPQ-Oct, and (l) ZnO_BDPQ-Oct_exf devices under UV LED illumination. Acetone gas sensing of (m) ZnO, (n) ZnO_BDPQ-Oct, and (o) ZnO_BDPQ-Oct_exf devices under white LED illumination. CO gas sensing of (p) ZnO, (q) ZnO_BDPQ-Oct, and (r) ZnO_BDPQ-Oct_exf devices under white LED illumination.

References

[S1] A. P. Dhondge, Y. X. Huang, T. Lin, Y. H. Hsu, S. L. Tseng, Y. C. Chang, H. J. H. Chen, and M. Y. Kuo, The Journal of Organic Chemistry 2019, 84, 14061-14068.

The AI processing procedure performs the following goals

1. Converts raw time-series sensor data (from two channels) into CNN-compatible samples using a **sliding window**.
2. Labels the data into **two classes** representing different gas conditions (or sources).
3. Builds a **1D Convolutional Neural Network (CNN)** for training and classification.

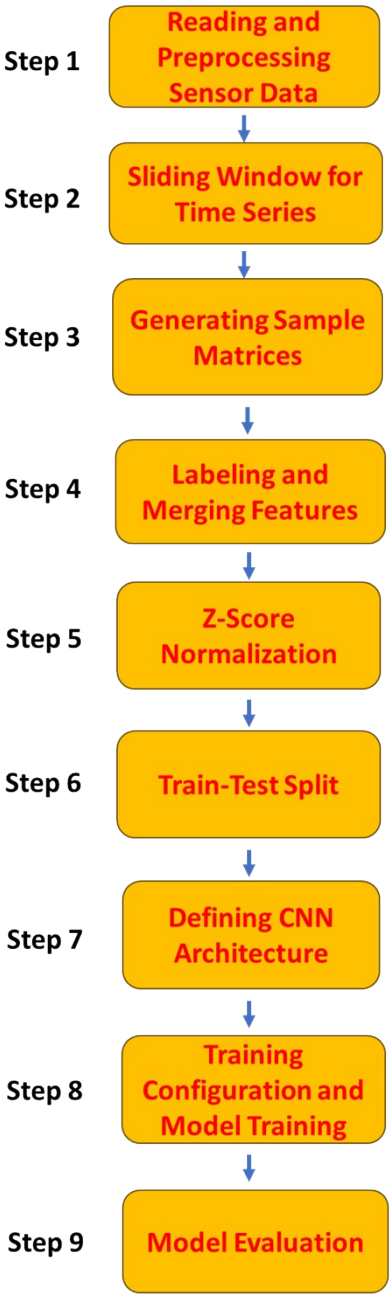

Figure. The practical operational steps of CNN model gas classifications.

4. Evaluates model performance using **accuracy** and **confusion matrices**.

CNN MODEL:

```
Ytrain = categorical(Ytrain);
Ytest = categorical(Ytest);

layers = [
   sequenceInputLayer(frame_size)
   convolution1dLayer(15, 15, 'Padding', 'same')
   reluLayer
   batchNormalizationLayer
   convolution1dLayer(15, 10, 'Padding', 'same')
   reluLayer
   batchNormalizationLayer
   convolution1dLayer(15, 5, 'Padding', 'same')
   reluLayer
   batchNormalizationLayer
   flattenLayer
   fullyConnectedLayer(2)
   softmaxLayer
   classificationLayer
];
```

Layer Description:

Layer Type	Function
sequenceInputLayer(...)	Input layer: 500-length time-series per sample.
convolution1dLayer(...) ×3	1D convolution: extracts local temporal features using varying filter sizes.
reluLayer	Non-linear activation to increase expressiveness.
batchNormalizationLayer	Normalizes data to accelerate and stabilize training.
flattenLayer	Flattens feature maps into 1D vector.
fullyConnectedLayer(2)	Final layer: outputs probabilities for 2 classes.
softmaxLayer + classificationLayer	Converts outputs to class probabilities and computes classification loss.

```
frame_shift = 25;
```

- y is the label vector: each sample is labeled as class 1 (from x1) or class 2 (from x2).
- size(X_1, 1): Number of samples from x1.
- X: Merged feature matrix, where each row is a 500-point sample.